Using a Family of Curves to Approximate the Pareto Front of a Multi-Objective Optimization Problem

Saúl Zapotecas Martínez[1], Víctor A. Sosa Hernández[2], Hernán Aguirre[1],
Kiyoshi Tanaka[1] and Carlos A. Coello Coello[2]

[1] Faculty of Engineering, Shinshu University, 4-17-1 Wakasato, Nagano, 380-8553, Japan
`saul.zapotecas@gmail.com,{ahernan,ktanaka}@shinshu-u.ac.jp`
[2] Computer Science Department, CINVESTAV-IPN, Av. IPN 2508, C.P. 07360,
San Pedro Zacatenco, Mexico D.F., Mexico
`msosa@computacion.cs.cinvestav.mx, ccoello@cs.cinvestav.mx`

Abstract. The design of selection mechanisms based on quality assessment indicators has become one of the main research topics in the development of Multi-Objective Evolutionary Algorithms (MOEAs). Currently, most indicator-based MOEAs have employed the hypervolume indicator as their selection mechanism in the search process. However, hypervolume-based MOEAs become inefficient (and eventually, unaffordable) as the number of objectives increases. In this paper, we study the construction of a reference set from a family of curves. Such reference set is used together with a performance indicator (namely Δ_p) to assess the quality of solutions in the evolutionary process of an MOEA. We show that our proposed approach is able to deal (in an efficient way) with problems having many objectives (up to ten objective functions). Our preliminary results indicate that our proposed approach is highly competitive with respect to two state-of-the-art MOEAs over the set of test problems that were adopted in our comparative study.

1 Introduction

In spite of the success of Multi-Objective Evolutionary Algorithms (MOEAs) for solving engineering and scientific problems, their application in problems with many objectives continues to be a hot research topic. In the last decade, several indicator-based MOEAs have been proposed [1,13,16]. The main motivation for using indicator-based MOEAs is that Pareto optimality quickly degrades its performance as we increase the number of objectives. One of the most popular indicator-based MOEAs of today is the *S Metric Selection Evolutionary Multi-Objective Algorithm (SMS-EMOA)* [1], which is based on the use of the hypervolume. However, SMS-EMOA has an important disadvantage: computing the hypervolume in high dimensionality (i.e., for problems with 4 or more objectives) is computationally expensive and quickly becomes unaffordable.

This has led to the use of other quality indicators such as: $R2$ [10] and Δ_p [14]. For these two indicators, it is possible to use a reference set in order to compute such metrics.[1] In fact, it is absolutely necessary the definition of a reference set for the Δ_p indicator. In the specialized literature, most authors working with indicator-based MOEAs,

---

[1] The version of $R2$ using a reference set is called $R2_R$ in [10].

have preferred the use of $R2$ (see e.g., [2,7,11]), while the use of Δ_p has been scarcely explored (see e.g. [8,13]). This is, perhaps, because it is easier to formulate a set of cost functions (another form of using $R2$) than to define a reference set (this requires an appropriate discretization of the real Pareto front). Since the features of the real Pareto front of a multi-objective optimization problem (MOP) are unknown, the construction of an appropriate reference set becomes a real challenge for the design of MOEAs based on reference sets. Some authors have defined the reference set by constructing segments of the possible Pareto front employing information of the nondominated solutions found along the search process, see e.g. [13]. Nonetheless, the construction of a generalized structure (a generalized reference set) constitutes a field still unexplored. In this paper, we propose the *Reference Indicator-Based Evolutionary Multi-Objective Algorithm (RIB-EMOA)*, which is based on Δ_p [14] and builds a reference set by using a family of curves. Our proposed approach is compared with respect to two other MOEAs using standard test problems having between three and ten objectives.

The remainder of this paper is organized as follows. In Section 2, we present the basic concepts required to understand this paper. In Section 3, we explain the general framework of our proposed approach. The detailed description of the construction of the reference set is presented in Section 4. In Section 5, we present the validation of our proposed approach. Finally, the conclusions and some possible paths for future research are drawn in Section 6.

2   Basic Concepts

2.1   Multi-objective Optimization

Assuming minimization, a continuous MOP can be formulated as:

$$\min_{\mathbf{x} \in \Omega} \quad F(\mathbf{x}) \tag{1}$$

where $\Omega \subset \mathbb{R}^n$ defines the decision space and $F : \Omega \to \mathbb{R}^k$ is defined as the vector of continuous functions, such that each $f_j : \Omega \to \mathbb{R}$ $(j = 1, \ldots, k)$ represents the function to be minimized. In this paper, we consider the box-constrained case, i.e., $\Omega = \prod_{i=1}^{n}[a_j, b_j]$. Therefore, each variable vector $\mathbf{x} = (x_1, \ldots, x_n)^T \in \Omega$ is such that $a_i \leq x_i \leq b_i$ for all $i \in \{1, \ldots, n\}$.

Definition 1.   *a) Let $\mathbf{x}, \mathbf{y} \in \Omega$. Then the vector $\mathbf{x}$ "dominates" $\mathbf{y}$ (denoted by $\mathbf{x} \prec \mathbf{y}$) with respect to the problem* (1)*, if and only if: i) $f_i(\mathbf{x}) \leq f_i(\mathbf{y})$ for all $i \in \{1, \ldots, k\}$; and ii) $f_j(\mathbf{x}) < f_j(\mathbf{y})$ for at least one $j \in \{1, \ldots, k\}$.*
  b) Let $\mathbf{x}^\star \in \Omega$, we say that $\mathbf{x}^\star$ is a "Pareto optimal" solution, if there is no other solution $\mathbf{y} \in \Omega$ such that $\mathbf{y} \prec \mathbf{x}^\star$.
  c) The Pareto set (PS) of problem (1) *is defined by: $PS = \{\mathbf{x} \in \Omega : \mathbf{x}$ is a Pareto optimal solution\} and the Pareto front (PF) is defined by: $PF = \{F(\mathbf{x}) : \mathbf{x} \in PS\}$.*

2.2 Δ_p Indicator

The Δ_p indicator [14], can be viewed as the Hausdorff distance between an approximation set and the real *PF* of a MOP. This indicator is defined by a slight modification

```
Input:                                          Input:
a stopping criterion;                           Q: the population to be reduced;
N: the population size;                          Output:
Output:                                         Q*: the reduced population.
Pt: the final approximation to the PF.      1   P* = nondominated_solutions(Q);
1  t = 0;                                     2   if P* ≠ Q then
   /* Initialize a population of N individuals */  3       s = arg max_{y∈Q}  d(y, Q);
2  Pt = {x¹,...,xᴺ};                          4   else
3  while stopping criterion is not satisfied do  5       s = arg max_{y∈Q}  Ψ(y, Q, R);
       /* Generate a trial solution       */  6   end
4      q = generate(Pt);                       7   Q* = Q \ {s};
       /* Select the N best individuals   */  8   return (Q*)
5      Pt+1 = reduce(Pt ∪ {q});
6      t = t + 1;
7  end
```

Algorithm 2: *reduce(Q)*

Algorithm 1: RIB-EMOA

from the well-known quality indicators: Generational Distance (GD) [15] and Inverted Generational Distance (IGD) [3]. Formally, the Δ_p indicator can be defined as follows.

Definition 2. *Let $P = \{x^1, \ldots, x^{|P|}\}$ an approximation and $R = \{r^1, \ldots, r^{|R|}\}$ be a discretization of the real PF of a MOP. The "Δ_p indicator" is defined as:*

$$\Delta_p(P, R) = \max\{I_{GD_p}(P, R), I_{IGD_p}(P, R)\} \tag{2}$$

where I_{GD_p} and I_{IGD_p} are a slight modification from GD and IGD, respectively. They are defined as: $I_{GD_p}(P, R) = \left(\frac{1}{|P|} \sum_{i=1}^{|P|} d_i^p\right)^{\frac{1}{p}}$ and $I_{IGD_p}(P, R) = \left(\frac{1}{|R|} \sum_{j=1}^{|R|} \hat{d}_j^p\right)^{\frac{1}{p}}$, where d_i and $\hat{d}_j$ are: the Euclidean distance from x^i to its closest member $r \in R$, and the Euclidean distance from r^j to its closest member $x \in P$, respectively.

Therefore, a low Δ_p value means that the set P has a better approximation to the real *PF*. More details of the Δ_p indicator and its properties can be found in [14].

3 The Reference Indicator-Based EMOA

3.1 General Framework

RIB-EMOA initializes a population P_t ($t = 0$) of N randomly generated individuals. A new individual q is generated by choosing (in a random way) two different parents from P. The parents are recombined by means of Simulated Binary Crossover (SBX) and the resulting children are mutated using Polynomial-Based Mutation (PBM) [5].[2] The new individual q (defined by any child) becomes a member of the next population P_{t+1}, if replacing another individual leads to a higher quality of the population in terms of the Δ_p indicator. The general framework of RIB-EMOA is presented in Algorithm 1. In the following sections, we will explain the reduction procedure (in Algorithm 1) and the proposed reference set construction procedure.

---

[2] However, the use of any other evolutionary operators is also possible.

3.2   Reduction Procedure

The procedure "*reduce*" (in Algorithm 1) selects the N best individuals from $Q = P_t \cup \{\mathbf{q}\}$ using the Δ_p indicator and a discretization of the real *PF* (denoted as R). In the following description, let us consider $P^\star$ and $d(\mathbf{y}, Q)$ as the set of nondominated solutions in Q and the number of points from Q that dominate solution $\mathbf{y} \in Q$, respectively. More formally, $d(\mathbf{y}, Q) = |\{\mathbf{x} \in Q : \mathbf{x} \prec \mathbf{y}, \mathbf{x} \neq \mathbf{y}\}|$. Since the cardinality of Q is $N+1$, one solution from Q needs to be discarded. The following definition is introduced.

Definition 3. *Let R be a discretization of the real PF of a MOP. The exclusive contribution of a solution $\mathbf{y} \in Q$ to the Δ_p indicator is defined as:*

$$\Psi(\mathbf{y}, Q, R) = \Delta_p(Q \setminus \{\mathbf{y}\}, R) \tag{3}$$

Clearly, if $P^\star = Q$, then all solutions in Q are nondominated and all of them are equally efficient in terms of Pareto optimality. In this case, we discard the solution $\mathbf{s} \in Q$ such that it maximizes the contribution to the Δ_p indicator, that is: $\mathbf{s} = \arg\max_{\mathbf{y} \in Q} \Psi(\mathbf{y}, Q, R)$. On the other hand, if $P^\star \neq Q$ then there exist solutions in Q dominated by any solution in $P^\star$. In this case, we discard the solution with the highest $d(\mathbf{y}, Q)$ value instead of using the Δ_p indicator. With that, the computation of Δ_p is avoided, thus reducing the computational cost of RIB-EMOA. Algorithm 2 shows the general *reduce* procedure.

Since we do not have any information related to the real *PF* of the MOP, the discretization of the reference set (R) is carried out by generating an artificial surface which should be a proper representation to the real *PF*. The next section will explain (in detail) the construction of such reference surface.

4   Reference Set Construction

4.1   Pareto Front Families

In real-world applications, there exist several problems for which the features of the real *PF* of a MOP are unknown. However, such *PF* could describe a convex or concave curve in objective space; otherwise, the *PF* could draw a linear surface where there is neither concavity nor convexity. Without loss of generality, we will assume that the *PF* of a MOP is normalized in the range $[0, 1]$, i.e., $0 \leq f_j \leq 1$, for each $j \in \{1, \ldots, k\}$. Then, we associate such *PF* to a curve of the following family:

$$\left\{ (y_1)^\alpha + \ldots + (y_k)^\alpha = 1 : y_j \in [0, 1], \alpha \in (0, \infty) \right\} \tag{4}$$

This family of curves possesses the following properties: 1) if $\alpha > 1$, the curve is concave; 2) if $\alpha < 1$, the curve is convex; and 3) if $\alpha = 1$, a linear surface is defined. Clearly, if $\alpha = 1$, then each vector $\mathbf{y}^i = (y_1^i, \ldots, y_k^i)^T$ in the surface satisfies $\sum_{j=1}^{k} y_j^i = 1$ and $y_j^i \geq 0$, for each $i \in \{1, \ldots, \mu\}$. In other words, if $\alpha = 1$, the surface will describe a set of weight vectors, which could be much easier to be discretized.

Remark 1. Let $C = \{\mathbf{c}^1, \ldots, \mathbf{c}^\mu\}$ be a set of μ weight vectors in $\mathbb{R}^k$, i.e., each $\mathbf{c}^i = (c_1^i, \ldots, c_k^i)^T$ satisfies $\sum_{j=1}^{k} c_j^i = 1$ and $c_j^i \geq 0$, for each $i \in \{1, \ldots, \mu\}$. Then, the vector:

$$\mathbf{y}^i = (c_1^i / \|\mathbf{c}^i\|_\alpha, \ldots, c_k^i / \|\mathbf{c}^i\|_\alpha)^T \tag{5}$$

satisfies equation (4), where $\| \cdot \|_\alpha$ denotes the α-norm function.
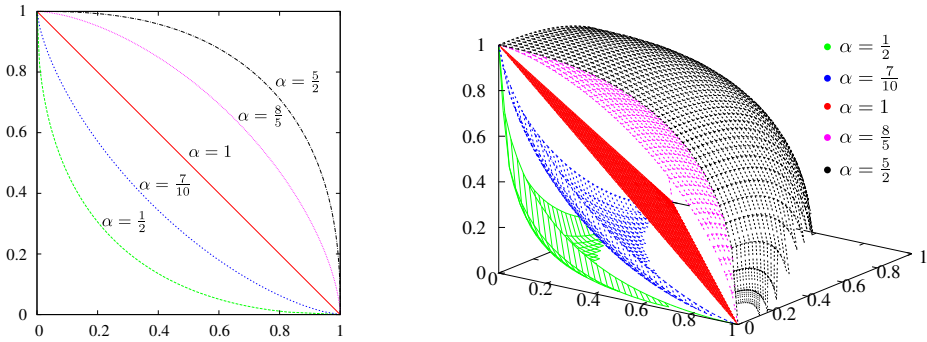
Fig. 1. Reference curves for $\alpha = \frac{1}{2}, \frac{7}{10}, 1, \frac{8}{5}, \frac{5}{2}$ in MOPs with two and three objective functions

The above remark motivates the construction of a set of weight vectors. Moreover, if the weight vectors are properly distributed in $\mathbb{R}^k$, a proper representation of the reference curve could be reached. Therefore, the weight set shall be the starting point for the construction of different curves by using equation (4). In Figure 1, we show different curves for different α values in problems with two and three objectives, respectively.

4.2 Weights Set

In the specialized literature, there are several strategies for generating weight vectors in an Euclidean space. Among these techniques, the Uniform Design (UD) method [9] has shown to be an effective technique in the design of weight vectors properly scattered. However, this technique becomes inefficient when the dimensionality (k) and the cardinality (μ) of the weights set increase; it has a computational complexity of $O\binom{\mu}{k}$. Since we use the reference surface (constructed from the weights set) to compute the Δ_p indicator, for a better quality of measurement, the number of elements in the discretized reference surface should be greater than the approximation to the PF given by the MOEA. Here, we generate the weights set by using a low discrepancy sequence based on lattices, whose complexity is given by $O(\mu \times k)$, which is far lower than the one given by the UD method.

Let d be the dimension of each vector in the low discrepancy sequence. Then, the ith vector in the sequence (for $i = 1, \ldots, \mu$) is defined by:

$$(i/k, \{i \times \rho_1\}, \ldots, \{i \times \rho_{d-1}\}) \tag{6}$$

where $\rho_1, \ldots, \rho_{d-1}$ are $d-1$ distinct irrational numbers and $\{\cdot\}$ denotes the fractional part of the real value (modulo-one arithmetic). In this work, we stated each ρ_l by the transcendental number $\varphi = \frac{\sqrt{5}+1}{2}$ (the golden section), i.e., $\rho_l = \varphi$ for each $l \in \{1, \ldots, d-1\}$.

Let $B^{k-1} = [0, 1]^{k-1}$ be the $(k-1)$-dimensional design space in a unit cube. Let $B^\star = \{\mathbf{b}^1, \ldots, \mathbf{b}^\mu\}$ be the lattice-based low discrepancy sequence on B^{k-1} generated by equation (6). Each weight vector $\mathbf{c}^i = (c_1^i, \ldots, c_k^i)^T \in C = \{\mathbf{c}^1, \ldots, \mathbf{c}^\mu\}$ is achieved by employing each $\mathbf{b}^i = (b_1^i, \ldots, b_{k-1}^i)^T \in B^\star$ according to the following equation:

$$c^i_j = \begin{cases} \left(1 - (b^i_j)^{\frac{1}{k-j}}\right) \prod_{l=1}^{j-1} (b^i_l)^{\frac{1}{k-l}}, & \text{if } j \in \{1, \dots, k-1\} \\ \prod_{l=1}^{k-1} (b^i_l)^{\frac{1}{k-l}}, & \text{if } j = k \end{cases} \qquad (7)$$

The above transformation, satisfies $\sum_{j=1}^{k} c^i_j = 1$, $c^i_j \geq 0$, for each $i \in \{1, \dots, \mu\}$ [9].

4.3   Reference Surface Construction

After obtaining the weights set (C), the reference surface is constructed by finding the α value that will transform the set C in an appropriate curve for a determined MOP. The following definition is relevant.

Definition 4. *Let $\mathbf{x}^\star_j$ be the respective global minimizers of $f_j(\mathbf{x})$, $j = 1, \dots, k$ over $\mathbf{x} \in \Omega$. Let $F^\star_j = F(\mathbf{x}^\star_j)$, $j = 1, \dots, k$. Let Φ be the $k \times k$ matrix whose j^{th} column is $F^\star_j - F^\star$. Then, the set of points in $\mathbb{R}^k$ that are convex combinations of $F^\star_j$, i.e., $\mathcal{H} = \{\Phi\beta : \beta \in \mathbb{R}^k, \sum_{j=1}^{k} \beta_j = 1, \beta_j \geq 0\}$ is referred to as the Convex Hull of Individual Minima (CHIM) [4].*

In the above definition, $F^\star = (f^\star_1, \dots, f^\star_k)^T$ denotes the utopian vector defined by the global minima values of each objective function f_j.

Let us consider $Q = P_t \cup \{\mathbf{q}\}$ as the current approximation to the real *PF* achieved by RIB-EMOA. Then, we state the extremes (individual minima) of the *PF* (denoted by ξ^i's, for each $i \in \{1, \dots, k\}$) according to the following achievement function.

$$\xi^i = \arg\min_{\mathbf{x} \in Q} \; \max_{j=1}^{k} \left((f_j(\mathbf{x}) - f^\star_j)/e^i_j \right) \qquad (8)$$

where $\mathbf{e}^i = (e^i_1, \dots, e^i_k)^T$ is the canonical basis in $\mathbb{R}^k$ (i.e., $\mathbf{e}^i$ denotes the vector with a 1 in the ith coordinate and 0 elsewhere). Each $f^\star_j$ is stated by the minimum value of the jth objective function found along the search process. For $e^i_j = 0$, we use $e^i_j = 1 \times 10^{-6}$.

Let us consider $H^b = (\mathbf{z}^b, \mathbf{n}^b)$ as the hyper box formed by the extreme vectors $\{\xi^1, \dots, \xi^k\}$. More precisely, the hyper box H^b is defined by the vectors $\mathbf{z}^b = (z_1, \dots, z_k)^T$ and $\mathbf{n}^b = (n_1, \dots, n_k)^T$, such that: $z_j = \min_{i=1}^{k} \xi^i_j$ and $n_j = \max_{i=1}^{k} \xi^i_j$, for each $j \in \{1, \dots, k\}$. Then, the computation of α for the creation of the reference surface takes place according to the following description.

Let $A = \{\mathbf{x}^1, \dots, \mathbf{x}^{|A|}\}$ be the set of nondominated solutions from Q such that each solution vector $F(\mathbf{x}^i) = (f_1(\mathbf{x}^i), \dots, f_k(\mathbf{x}^i))^T$ is contained in the hyper box H^b. We consider that each solution vector $F(\mathbf{x}^i)$ is normalized in $[0, 1]$, and it will be denoted as $\hat{F}(\mathbf{x}^i) = (\hat{f}_1(\mathbf{x}^i), \dots, \hat{f}_k(\mathbf{x}^i))^T$, for each $i \in \{1, \dots, |A|\}$. Then, the convex hull $\mathcal{H}$ in the normalized space corresponds to be a set of weight vectors and we denote to this as $\hat{\mathcal{H}}$.

The α value is stated by finding the solution vector $\hat{F}(\mathbf{x}^b)$ which describes the maximum bulge (sometimes called "knee") formed by the convex hull $\hat{\mathcal{H}}$ and the solution vectors $\hat{F}(\mathbf{x}^i)$'s. We state this solution $(\mathbf{x}^b)$ such that it minimizes a Tchebycheff problem. To be more precise: $\mathbf{x}^b = \arg\min_{\mathbf{x} \in A} \; \max_{1 \leq j \leq k} \{\lambda_j | \hat{f}_j(\mathbf{x}) - f^\star_j |\}$ with the weight vector $(\lambda_1 = \frac{1}{k}, \dots, \lambda_k = \frac{1}{k})^T$, where k denotes the number of objective functions.

In order to ensure that the reference curve will touch the maximum bulge, it is initially defined by finding the α value which satisfies equation (4) for the solution vector $\hat{F}(\mathbf{x}^b)$. In other words:[3] $\alpha = \arg\min_{\hat{\alpha}\in(0,\infty)} \hat{f}_1(\mathbf{x}^b)^{\hat{\alpha}} + \cdots + \hat{f}_k(\mathbf{x}^b)^{\hat{\alpha}} - 1$.

Let us consider the weights set C as an appropriate discretization of $\hat{\mathcal{H}}$. Then, the construction of the reference surface $R = \{\mathbf{y}^1, \ldots, \mathbf{y}^\mu\}$ is carried out by transforming each weight vector $\mathbf{c}^i \in C$ according to equation (5), for each $i \in \{1, \ldots, \mu\}$. This transformation does not guarantee that all the elements in R dominate to all solution vectors $\hat{F}(\mathbf{x}^i)$, for each $\mathbf{x}^i \in A$. However, since the surface (R) intersects the maximum bulge (i.e., it passes through the point $\hat{F}(\mathbf{x}^b)$) and all solutions in A are nondominated, most solutions in A should be dominated by R. Nevertheless, the reference surface is fixed to dominate all the solutions in A.

For each solution vector $\hat{F}(\mathbf{x}^i)$ there exists a vector $\mathbf{h}^i = (h_j^i, \ldots, h_k^i)^T$ with direction $\hat{F}(\mathbf{x}^i)$ (from the origin) such that $\mathbf{h}^i$ is a weight vector, i.e., $\mathbf{h}^i \in \hat{\mathcal{H}}$. Such weight vector can be reached by $h_j^i = \hat{f}_j(\mathbf{x}^i)/\sum_{j=1}^k \hat{f}_j(\mathbf{x}^i)$, for each $i \in \{1, \ldots, |A|\}$ and $j \in \{1, \ldots, k\}$. Then, before computing the transformation of the whole weights set, we verify if $\mathbf{h}^i$ under the transformation of α in equation (5) (denoted by $\mathbf{h}_\alpha^i$) is dominated by $\hat{F}(\mathbf{x}^i)$. In such case (i.e., if $\hat{F}(\mathbf{x}^i) \prec \mathbf{h}_\alpha^i$), a new search of α needs to be conducted, but using the solution vector $\hat{F}(\mathbf{x}^i)$ instead of $F(\mathbf{x}^b)$. Finally, the normalized surface R is translated to the utopian vector $F^\star$ and scaled to the individual minima ξ's, i.e., in the original objective space.

5   Experimental Study

In order to assess the performance of our proposed approach, we compared its results with respect to those obtained by SMS-EMOA and a version of SMS-EMOA that uses Monte Carlo simulations to approximate the S metric (we called it HyPE-EMOA). We adopted the seven unconstrained MOPs from the well-known DTLZ test suite [6]. Due to space limitations and the known geometrical shapes of each DTLZ problem, we compare herein, the performance of each algorithm by using only the Generational Distance (GD) [15]. The GD for DTLZ1 was computed as $GD = \frac{1}{|P|} \sum_{\mathbf{x}\in P} \|F(\mathbf{x})\|_1 - 0.5$ since its PF is a hyperplane that intersects each axis in 0.5. For DTLZ2-DTLZ4 we used $GD = \frac{1}{|P|} \sum_{\mathbf{x}\in P} \|F(\mathbf{x})\|_2 - 1$ since the PF for theses problems describes a sphere of radius 1. For DTLZ5-DTLZ7, we used the value of each auxiliary function $g(\mathbf{x})$ defined for each
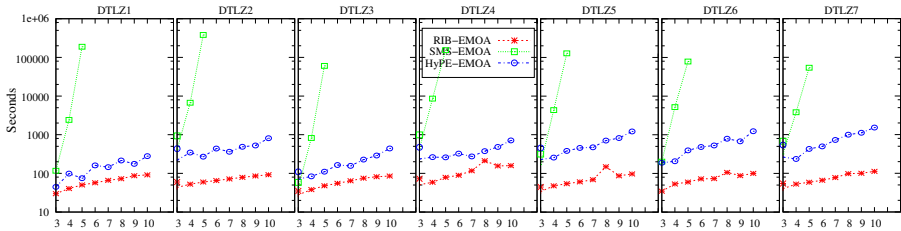

Fig. 2. Average time (axis y) over 30 independent runs for each MOEA when performing 40,000 functions evaluations for each DTLZ test problem (from 3 to 10 objectives functions (axis x))

---

[3] We find out the α value by using the golden search method [12] within the interval $(0.05, 20)$.

problem (for details see [6]). The *PF* of DTLZ5 and DTLZ6 is achieved when $g(\mathbf{x}) = 0$, while the *PF* of DTLZ7 is reached when $g(\mathbf{x}) = 1$. Thus, we used each g function to compute a variant of *GD*, defined by $GD_g = \frac{1}{|P|} \sum_{\mathbf{x} \in P} g(\mathbf{x})$ (for DTLZ5 and DTLZ6) and $GD_g = \frac{1}{|P|} \sum_{\mathbf{x} \in P} g(\mathbf{x}) - 1$ (for DTLZ7), where P denotes the final approximation achieved by each MOEA. Therefore, a value $GD = 0$ indicates that the approximation P is in the real *PF*. For each algorithm, we used $\eta_c = 15, \eta_m = 20, p_c = 0.9$ and $p_m = 1/n$ for the indexes and ratios in the crossover and mutation operators, respectively. For each MOP,

Table 1. Comparison of results with respect to *GD* for the DTLZ test problems

# Objs.	Algorithm	DTLZ1 GD (σ)	DTLZ2 GD (σ)	DTLZ3 GD (σ)	DTLZ4 GD (σ)	DTLZ5 GD (σ)	DTLZ6 GD (σ)	DTLZ7 GD (σ)
3	RIB-EMOA	0.004213 (0.005947)	**0.000041** (0.000048)	17.487000 (7.263660)	**0.000029** (0.000045)	**0.000001** (0.000003)	3.877700 (0.173200)	**0.001201** (0.000394)
	SMS-EMOA	**0.001780** (0.001996)	0.000065 (0.000011)	12.160000 (4.633868)	0.000043 (0.000016)	0.000003 (0.000001)	**2.617500** (0.067991)	0.001615 (0.000177)
	HyPE-EMOA	0.029672 (0.023956)	0.000458 (0.000071)	**12.147000** (5.979108)	0.000363 (0.000165)	0.000040 (0.000011)	4.459300 (0.138107)	0.016254 (0.001617)
4	RIB-EMOA	0.037965 (0.049938)	**0.000155** (0.000085)	18.517000 (7.833201)	**0.000107** (0.000197)	**0.000004** (0.000007)	8.367200 (0.841955)	0.036396 (0.016740)
	SMS-EMOA	**0.001861** (0.001276)	0.000201 (0.000025)	**17.132000** (8.927643)	0.000115 (0.000047)	0.571280 (0.023577)	**3.306000** (0.092850)	**0.007434** (0.000678)
	HyPE-EMOA	0.977570 (1.153816)	0.001886 (0.000293)	64.291000 (18.986294)	0.001209 (0.000301)	0.296780 (0.045810)	9.936200 (0.358386)	0.122510 (0.025145)
5	RIB-EMOA	0.029738 (0.027467)	**0.000316** (0.000147)	13.776000 (7.468234)	**0.000536** (0.000226)	**0.004092** (0.009992)	10.489000 (0.639423)	0.157760 (0.045098)
	SMS-EMOA	**0.002510** (0.001591)	0.000415 (0.000056)	**9.849800** (2.726240)	0.000656 (0.000036)	0.787580 (0.053845)	**3.374800** (0.082385)	**0.014730** (0.001261)
	HyPE-EMOA	1.929400 (1.138770)	0.005508 (0.000839)	83.570000 (16.132044)	0.003014 (0.000682)	0.330560 (0.043337)	11.866000 (0.346546)	0.307590 (0.059810)
6	RIB-EMOA	**0.097693** (0.144339)	**0.000809** (0.000255)	**20.824000** (11.602267)	**0.000887** (0.000321)	**0.041967** (0.057430)	**12.185000** (0.569374)	**0.128210** (0.080949)
	HyPE-EMOA	2.018500 (1.313371)	0.011268 (0.001611)	98.789000 (21.181272)	0.005243 (0.001365)	0.348890 (0.026693)	13.047000 (0.322326)	0.477420 (0.115235)
7	RIB-EMOA	**0.374010** (0.525594)	**0.001308** (0.000443)	**26.081000** (14.997568)	**0.001996** (0.000985)	**0.065241** (0.103754)	**13.460000** (0.480379)	**0.122180** (0.041164)
	HyPE-EMOA	2.409300 (1.449388)	0.017296 (0.002415)	99.057000 (19.874297)	0.009122 (0.002152)	0.362480 (0.032717)	13.732000 (0.309724)	0.670290 (0.119358)
8	RIB-EMOA	**0.493850** (0.739671)	**0.001746** (0.000450)	**26.249000** (14.347574)	**0.006156** (0.002254)	**0.082622** (0.071311)	**14.323000** (0.283957)	**0.187260** (0.066961)
	HyPE-EMOA	2.451000 (1.522215)	0.023798 (0.003426)	105.050000 (23.295721)	0.017033 (0.004348)	0.380640 (0.036984)	14.494000 (0.247828)	1.020500 (0.090525)
9	RIB-EMOA	**0.459380** (0.491440)	**0.004350** (0.002952)	**26.887000** (16.594691)	**0.012242** (0.003688)	**0.093066** (0.080599)	**14.655000** (0.384037)	**0.267120** (0.077010)
	HyPE-EMOA	2.142300 (1.183025)	0.031247 (0.006355)	105.460000 (24.807379)	0.026099 (0.004833)	0.376190 (0.029685)	14.657000 (0.233302)	1.458500 (0.086545)
10	RIB-EMOA	**0.312500** (0.366907)	**0.008835** (0.004312)	**30.731000** (16.845582)	**0.018094** (0.006016)	**0.118400** (0.097462)	**15.062000** (0.371148)	**0.446840** (0.126770)
	HyPE-EMOA	2.574600 (1.366155)	0.034142 (0.005567)	109.580000 (19.801898)	0.039354 (0.010316)	0.398900 (0.026573)	15.090000 (0.297923)	1.962400 (0.086160)

30 independent runs were performed with each algorithm. We employed a population size N = 200 and the search was restricted to 40,000 fitness function evaluations for each problem. The cardinality of the reference set was set as $\mu = \rho \times N$ (here, we used ρ = 3). The results obtained are summarized in Table 1. This table displays both the *average* and the standard deviation (σ) for the *GD* performance measure for each MOP. For an easier interpretation, the best results are presented in **boldface**.

In our study, we tested the abilities of RIB-EMOA using our proposed reference set construction when solving MOPs with many objectives (between three and ten objective functions). From Table 1, we can see that RIB-EMOA obtained better approximations to the real *PF* than HyPE-EMOA in most of the test problems. Nevertheless, SMS-EMOA obtained better results than RIB-EMOA for DTLZ1, DTLZ3 and DTLZ6 test problems. The poor performance of RIB-EMOA in these problems could be due to the high multi-modality (in the case of DTLZ1 and DTLZ3) and the degeneration (in the case of DTLZ6) that these problems have in their *PF*s. Although DTLZ5 also has a degenerate *PF*, it is much more difficult to approximate solutions to the real *PF* of DTLZ6 than to the real *PF* of DTLZ5 (for details of these problems see [6]). In fact, RIB-EMOA relies on the proper construction of the reference set which is constructed from the individual minima of each problem. Thus, given the features of these MOPs, the achievement function (in equation (8)) which establishes the individual minima could be not the best in order to construct a proper surface for them. Nonetheless, an improvement mechanism for our proposed reference set construction, is indeed, a possible path for future research. On the other hand, according to Fig. 2, we can see that SMS-EMOA achieved good results for DTLZ1, DTLZ3 and DTLZ6 (see Table 1) but consuming a higher computational time than RIB-EMOA. However, the computational time required by our RIB-EMOA was lower than that of SMS-EMOA and HyPE-EMOA even when solving MOPs with 10 objective functions. Moreover, the time consumption for SMS-EMOA was so high that we could only test it with MOPs having up to 5 objectives. Based on the previous discussion, we consider that our proposed approach is a good choice in order to deal with MOPs with a high number of objectives.

6   Conclusions and Future Work

In this paper, we have presented a first attempt to generalize a reference set for a given MOP. For this sake, we have considered the fact that the *PF* of a MOP could be described as a linear, convex, or concave manifold in the objective function space. In such cases, the *PF*s present geometries which can be associated to a curve of the family described in equation (4). The proposed reference set construction was found to be appropriate, since it yields a suitable surface in order to approximate solutions to the real *PF* by using the $\mathit{\Delta}_p$ indicator (however, it could also be used with other MOEAs that adopt a reference set). According to our results, we showed the potential of our proposed approach for attracting solutions towards the real *PF* along the search process. It is indeed desirable to compare our proposed approach against more state-of-the-art MOEAs and this will be part of our future work. It is worth noting that our RIB-EMOA produced competitive results even with respect to problems having non-well-defined *PF*s (e.g., in DTLZ5-DTL7 (these MOPs have discontinuities and degenerations in their *PF*s)), which could be a useful feature when dealing with real-world MOPs.

As part of our future research, we intend to focus on designing another strategy in order to improve the construction of the reference set. It is also desirable to introduce the use of preferences to our proposed approach. Finally, we also aim to extend our proposed approach to deal with constrained MOPs having many objectives, which is an area that has remained practically unexplored so far, to the authors' best knowledge.

References

1. Beume, N., Naujoks, B., Emmerich, M.: SMS-EMOA: Multiobjective selection based on dominated hypervolume. EJOR 181(3), 1653–1669 (2007)
2. Brockhoff, D., Wagner, T., Trautmann, H.: On the properties of the R2 indicator. In: GECCO 2012, pp. 465–472. ACM (2012)
3. Coello Coello, C.A., Cruz Cortés, N.: Solving Multiobjective Optimization Problems using an Artificial Immune System. Genetic Programming and Evolvable Machines 6(2), 163–190 (2005)
4. Das, I.: Nonlinear Multicriteria Optimization and Robust Optimality. PhD thesis, Rice University, Houston, Texas (1997)
5. Deb, K., Pratap, A., Agarwal, S., Meyarivan, T.: A Fast and Elitist Multiobjective Genetic Algorithm: NSGA-II. IEEE TEVC 6(2), 182–197 (2002)
6. Deb, K., Thiele, L., Laumanns, M., Zitzler, E.: Scalable Test Problems for Evolutionary Multiobjective Optimization. In: Ajith, A., et al. (eds.) Evolutionary Multiobjective Optimization. Theoretical Advances and Applications, pp. 105–145. Springer, USA (2005)
7. Diaz-Manriquez, A., Toscano-Pulido, G., Coello Coello, C.A., Landa-Becerra, R.: A ranking method based on the R2 indicator for many-objective optimization. In: CEC 2013, pp. 1523–1530. IEEE (2013)
8. Dominguez-Medina, C., Rudolph, G., Schutze, O., Trautmann, H.: Evenly spaced pareto fronts of quad-objective problems using psa partitioning technique. In: CEC 2013, pp. 3190–3197. IEEE (2013)
9. Fang, K.T.: The Uniform Design: Application of Number-Theoretic Methods in Experimental Design. Acta Math. Appl. Sinica 3, 363–372 (1980)
10. Hansen, M.P., Jaszkiewicz, A.: Evaluating the quality of approximations to the non-dominated set. Technical Report IMM-REP-1998-7, Institute of Mathematical Modeling, Technical University of Denmark (1998)
11. Hernandez Gomez, R., Coello Coello, C.A.: MOMBI: A new metaheuristic for many-objective optimization based on the R2 indicator. In: CEC 2013, pp. 2488–2495. IEEE (2013)
12. Kiefer, J.: Sequential minimax search for a maximum. Proceedings of the American Mathematical Society 4(3), 502–506 (1953)
13. Rodríguez Villalobos, C.A., Coello Coello, C.A.: A new multi-objective evolutionary algorithm based on a performance assessment indicator. In: GECCO 2012, pp. 505–512. ACM (2012)
14. Schütze, O., Esquivel, X., Lara, A., Coello Coello, C.A.: Using the averaged Hausdorff distance as a performance measure in evolutionary multi-objective optimization. IEEE TEVC 16(4), 504–522 (2012)
15. Veldhuizen, D.A.V.: Multiobjective Evolutionary Algorithms: Classifications, Analyses, and New Innovations. PhD thesis, Department of Electrical and Computer Engineering. Graduate School of Engineering. Air Force Institute of Technology, Wright-Patterson AFB, Ohio (May 1999)
16. Zitzler, E., Künzli, S.: Indicator-based selection in multiobjective search. In: Yao, X., et al. (eds.) PPSN 2004. LNCS, vol. 3242, pp. 832–842. Springer, Heidelberg (2004)